Chapter 6

Electrochemical Deposition of P3AT Films Used as a Probe of Optical Properties in Polymeric System

Sankler Soares de Sá, Fernando Costa Basílio, Henrique de Santana, Alexandre Marletta and Eralci Moreira Therézio

Additional information is available at the end of the chapter

http://dx.doi.org/10.5772/66921

Abstract

Poly(3-alkylthiophene) (P3ATs) have been extensively used in photovoltaic devices such as a p-type organic Semiconductors. However, several electronic properties of P3ATs present energy transfer inter- and intra-chains that have direct consequences on the performance of optoelectronic devices. Traditionally electrochemical techniques, such as cyclic voltammetry, chronoamperometry and chronocoulometry, have been applied to process polymer thin films and unconventional spectroscopy techniques are used to characterize the electronic properties. In the present work, we used an innovative technique called ellipsometry emission to investigate the optical properties of P3AT films. We propose a new approach to study the electrochemical synthesize and unintentional doping processes of polymeric systems. We showed a strong correlation between the electrochemical synthesis and the optical properties controlling the film growth conditions for P3ATs. The results obtained in the present study can be potentially utilized for applications in organic devices, mainly in photovoltaic cells when the film deposition and the optical properties control are relevant.

Keywords: poly(3-alkylthiophene), electrochemical synthesis, optical properties, energy transfer, emission ellipsometry

1. Introduction

Over the last decades, semiconductor polymers have attracted considerable interest, particularly for the production of organic electroluminescent diodes (OLEDs) and organic photovoltaic cells (OPVs), in which they present high emission efficiency in the visible region and UV-Vis absorption in the broad spectral window [1, 2]. Devices using conductive polymers

exhibit some advantages over inorganic semiconductors. They are easily deposited on thin solid films by low-cost techniques such as spin coating, casting or electrochemical [2, 3]. Among the wide variety of conductive polymers, poly(3-*alkylthiophene*) (P3AT) has been studied due to its various physical-chemistry characteristics, e.g., good chemical stability, solubility (making it an easy deposition material on substrates) and has electrochromic and thermochromic characteristics [4]. Besides these properties, the luminescence efficiency of this polymer has increased significantly in the function of the *alkyl* chain length [5, 6]. Basically, P3ATs are the derivatives of polythiophene (PT) which are obtained from the polymerization of thiophene (monomer), a sulfur heterocyclic ring [7]. The precursor monomer of P3ATs, 3-*alkylthiophene* is also composed of thiophene ring and alkyl groups, in compliance with the following combination [5]:

$$C_n H_{2n+1} \tag{1}$$

where C is the carbon chemical element, H is the hydrogen chemical element and n is the number of carbons that compose the molecule.

The P3ATs chemically synthesized presented an energy *gap* of around 1.93 eV (640 nm) [5, 6, 8–12]. Interestingly, this *energy gap* independent of the size of the *alkyl* lateral chain because it is not conjugated. Therefore, the recombination of excited carriers occurs only in the main conjugated polymer chain. However, the intensity of the emission band is directly related to the alkyl chain [6]. Another important observation about the emission band intensity is the anomalous temperature dependence [5].

Ohmori et al. [6] have observed luminescence intensity dependence in function of the length of the *alkyl* chain. They used three P3ATs with different sizes of the *alkyl* chain. The P3ATs have traditionally been prepared by chemical synthesis from 3-AT monomers with $FeCl_3$ as a catalyst. Chemical synthesis of P3AT polymer, using a standard way in the literature, was first obtained by Yoshino et al. in 1984 [13]. In addition, Yoshino et al. [5] noted that the photoluminescence intensity (PL) of P3AT films increases in the function of the sample temperature and decreases after the melting point. This result has been discussed in terms of the effective conjugation length, since the dynamics of the excited species are influenced by the occurrence of a twist between the vicinity of the thiophene rings together with the interchain interaction. In the last decade, the interest in the organic electronic devices has increased significantly; however, some effects on their operation are not fully understood, in particular the interface effects of the substrate/polymer and energy transfer of excited carriers [9, 14–16]. Since the physical-chemistry properties and investigation of organic active layers, such as P3ATs thin solid films, can elucidate the development of new optoelectronic devices [16–18]. Interface effects cause significant quenching of excited carriers and it is commonly investigated by conventional spectroscopic techniques [15, 19], such as ultraviolet-visible absorption (UV-Vis), photoluminescence (PL), photoluminescence excitation (PLE), vibrational spectroscopy (FT-IR and RAMAN) [8, 12, 20, 21] and the morphological technique of atomic force microscopy (AFM) [22–24]. In the case of energy transfer processes of excited carriers, the analysis of polarization of emitted light can be directly correlated with polymeric chain position parallel to the direction of the transition dipole moment [25–27]. Moreover, we need to consider the effects of the deposition method.

In present work, we used the electrochemical synthesis for deposition of P3AT thin solid film correlating with optical properties. We demonstrated an easy and efficient alternative method

http://dx.doi.org/10.5772/66921

to control the processing of organic optoelectronic devices. In that context, Therézio et al. in [8] show two distinct structures of the polymer chain morphology shifting the band gap to higher energies, using an optical analysis of P3ATs films electrochemically prepared. Moreover, reference [9] also indicated that it is possible to analyze the polarization of the emitted light by the supporting electrolyte effects on the emission properties of P3ATs films. The results conclude quantitatively that the best-supporting electrolyte concentration for the P3ATs film's production is 0.100 mol L^{-1}. It is in absolute agreement of the electrolyte concentration used in the literature to P3ATs synthesis. Recently, Santana and coworkers [10, 12, 28, 29] have shown that the P3ATs synthesis is possible using different supporting electrolytes, solvents and thicknesses. Therefore, it was possible to correlate the growth conditions of the electrochemical synthesis and optical properties to produce polymer films with possible application in optoelectronic devices. We present the systematic study of two sets of poly(3-dodecylthiophene) (P3DDT) films grown electrochemically with two different electrolytes. All thin films were deposited on a transparent electrode FTO (fluorine-doped tin oxide) and cycles ranging from 1 to 10 cycles. In addition, it was possible to obtain the emission optical characteristics in the function of the amount of polymer deposited or the polymeric film thickness. We used, in the present investigation, UV-Vis absorption, photoluminescence and ellipsometry emission. As a result, we assign the use of an alternative optical characterization to probe the organic semiconductors obtained via electrochemical techniques [20, 23].

2. Electrochemical deposition in poly(3-alkylthiophenes) films

P3DDT samples were deposited on the FTO substrate by the electrochemical synthesis of 3-dodecylthiophene ($C_{16}H_{28}S$) monomer in an electrolyte solution containing a solvent, salt and monomer. In stoke solution, we used acetonitrile (CH_3CN), monomer 3-dodecylthiophene and lithium perchlorate ($LiClO_4$) or tetraethylammonium tetrafluoroborate ($((C_2H_5)_4NBF_4$ or Et_4NBF_4) salts [9]. The concentrations used are 0.100 mol L^{-1} for the support electrolyte (SE), 0.050 mol L^{-1} for the monomer and 0.040 mol L^{-1} for Et_4NBF_4 or $LiClO_4$ electrolyte. The options for the previous concentrations is based on the literature for poly(3-methylthiophene) and poly(3-octylthiophene) [9, 10, 30–32]. The films grown in the present study are labeled in **Table 1**.

2.1. Cyclic voltammetry

The P3DDT films were electropolymerized and deposited on FTO substrates by cycles of the voltammetry method (CV) using the IVIUM COMPACTSTAT potentiostat/galvanostat. Alternatively, reference [9] presented additional deposition techniques of chronoamperometry and chronocoulometry used to synthesize P3AT films [9]. Polymerization was accomplished by continuous cycling the potential of the FTO electrode between +2.200 and -0.000 V for Et_4NBF_4 and +2.900 and -1.000 V for $LiClO_4$. Electropolymerization scan rate was determined at 0.050 V/s. Different sample thicknesses were obtained by increasing the number of cycles in CV ranging from 1 to 10 for each electrolyte. In the electropolymerization CV technique, we used standard-three-electrodes-cells: platinum auxiliary electrode, reference electrode containing saturated demonized water solution of potassium chloride (KCl) and FTO-working electrode. Electrodes were immersed in an electrolyte solution containing acetonitrile, monomer 3-dodecylthiophene and inert salt under a controlled atmosphere using argon gas.

Electrolyte	Number of cycles	Nomenclature used
Et_4NBF_4	1	EtNBF01
	2	EtNBF02
	4	EtNBF04
	6	EtNBF06
	8	EtNBF08
	10	EtNBF10
$LiClO_4$	1	LiClO01
	2	LiClO02
	4	LiClO04
	6	LiClO06
	8	LiClO08
	10	LiClO10

Table 1. Label of P3DDT film in function of the cycles number and electrolyte.

Initially, the voltammetry cyclic synthesis, oxidate or reducte the polymer monomers bonding its covalently increasing the main chain length and deposit the polymer via physical-chemistry interaction with the working electrode. The polymer chain length formed in this process occurs until the saturation limit of the chain is achieved. Then, in each CV cycle new polymer chains are deposited on the previously deposited polymer layer. **Figure 1** shows the cyclic voltammogram for EtNBF10 (**Figure 1a**) and LiClO10 (**Figure 1b**) films. We observe that between the first and the last cycles, there are different maximum of reduction potentials 0.56 and 0.32 V for EtNBF10 and 0.36 and 0.48 V for LiClO10, respectively. These ddp differences indicate the film thickness and material deposited amount is increasing between consecutive CV cycles [33].

The increase in number of electropolymerization cycles leads to the formation of various layers until the saturation point of the film. Assuming that in each cycle, the maximum voltage of oxidation or reduction represents the cathode and anodic ionizing potential, respectively, the difference in ionization potentials allows us to infer the *energy gap* (E_g) of the material. It is important to observe that the CV curves need to display only one oxidation or reduction process, as in the case of P3DDT films, see **Figure 1**. This method was first introduced by Eckhardt et al. [34] for organic semiconductor materials. **Table 2** shows the oxidation and reduction maximum values for all P3DDT films. Calculated E_g values increase from the first to the last cycle regardless of the electrolyte since the resistance of the carriers is greater for the additional P3DDT layer after each cycle, thus increasing film thickness [30, 33].

By comparing the values, shown in **Table 2** for the *energy gap*, it can be observed that the films with the Et_4NBF_4 electrolyte require less energy for their formation. The increase in voltage required for the formation of films and of energy is due to the presence of BF_4^- and ClO_4^- anions in the electropolymerization, which has great influence on the morphology, structure and

http://dx.doi.org/10.5772/66921

electrochemical polymer properties [7–9, 19, 20, 31]. In addition, great E_g can be correlated with the high doping of P3DDT chains producing higher polymer quinone form. It was showed by Therézio et al. [8, 19] studied that the energy gap in doped P3AT films increases. Therefore, in our study, we also recommend the P3DDT films with lesser deposition cycles and lesser doped or lower *gap energy* which displays major polymer chains in the pristine form.

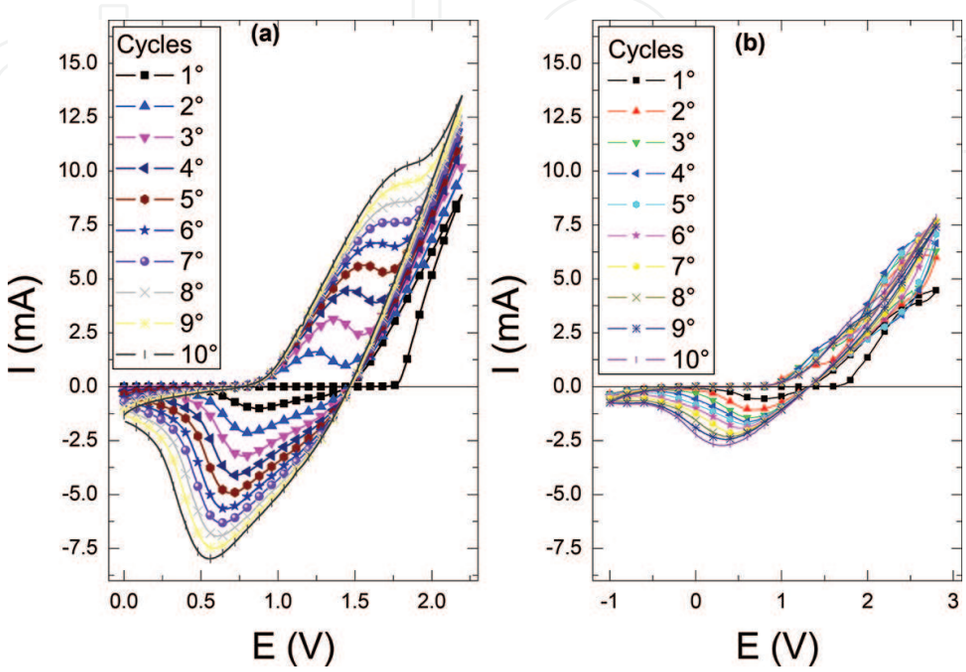

Figure 1. Cyclic voltammetry of (a) EtNBF10 and (b) LiClO10 films.

Film	Cathodic maximum (V)	Anodic maximum (V)	E_g (V)
EtNBF01	–	0.84	–
EtNBF02	1.25	0.80	0.45
EtNBF04	1.44	0.70	0.74
EtNBF06	1.62	0.68	0.94
EtNBF08	1.76	0.55	1.21
EtNBF10	1.82	0.55	1.27
LiClO01	2.40	0.84	1.56
LiClO02	2.55	0.68	1.87
LiClO04	2.61	0.64	1.97
LiClO06	2.80	0.59	2.21
LiClO08	2.80	0.45	2.35
LiClO10	2.80	0.30	2.50

Table 2. Cathodic and anodic ionization potential for P3DDT films.

3. Optical characterizations

3.1. UV-Vis absorption[1]

In the UV-Vis spectral range with maximum absorption centered at ~450 nm. For the EtNBF02 film, a well-resolved absorbance band at ~775 nm is also observed. This band is the result of the interaction between the BF_4^- anion and P3DDT polymer chains [8, 9, 20]. Similar results are observed in different P3AT polymers [35–37]. To higher electropolymerization cycle number, the band at ~775 nm is further evident (not shown), in which it is possible to correlate the cycle number and UV-Vis absorption intensity to follow the polymer-grown deposition. **Figure 2b** shows the absorption spectra for the LiClO01 and LiClO02 films in the UV-Vis spectral range. It observes in **Figure 2b** that the maximum absorption is approximated at ~400 nm for the LiClO02 film, but it cannot be confirmed by the exact spectral position because of the absorption of the FTO substrate. The blue shift of the absorption maximum position in comparison of absorbance spectra of the Et_4NBF_4 films should be considered due to the presence of two different P3DDT molecules morphologies or the diminish of the length of the polymer chains. As a result, the decrease of the conjugation and the increase of the gap energy of the material occur. That effect was recently reported by Therézio et al. [8, 12] to the P3AT derivative where the maximum position and intensity of absorption change in function of the electrolyte. Other castellation is the exposition of the film on the atmosphere environment that induces relatively quick (days) polymer films degradation. Lower intensity and poorly resolved absorbance band at ~650 nm is observed in **Figure 2b** for LiClO02 and thick films (not shown) due to the interaction between the ClO_4^- anions and the P3DDT molecules [8, 9, 12, 20, 31].

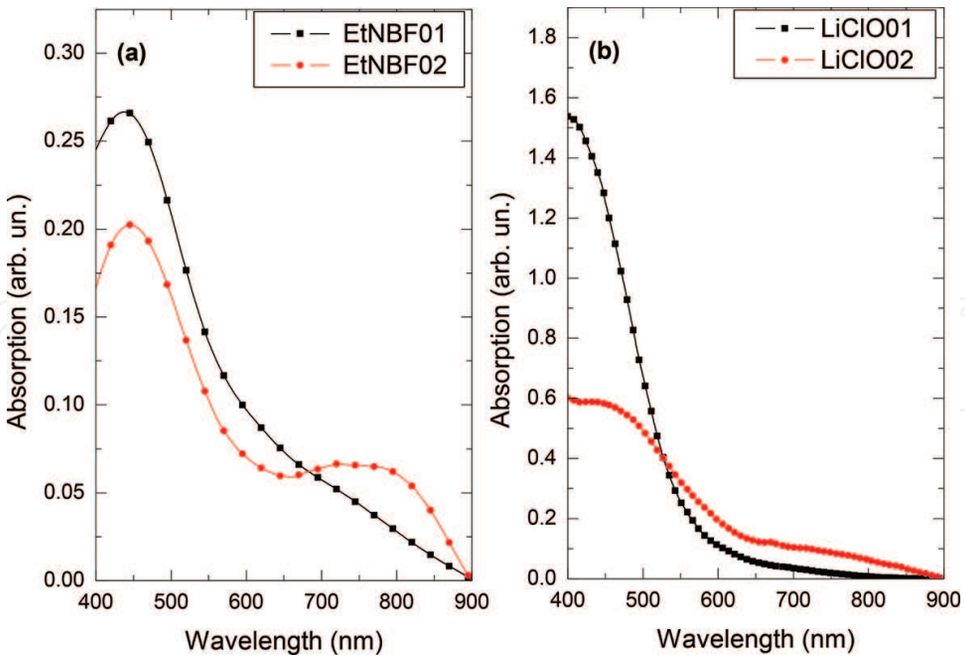

Figure 2. UV-Vis spectra for P3DDT films with one and two electropolymerization cycles: (a) EtNBF01 and EtNBF02 films and (b) LiClO01 and LiClO02 films.

[1]UV-Vis measurements were conducted using a spectrophotometer FEMTO XI 800, operating in the 190-900 nm range.

http://dx.doi.org/10.5772/66921

3.2. Photoluminescence (PL)[2]

We consider several radiative contributions associated with different interactions to simulate the emission spectra due to the presence of the anion in the electrolyte solution and polymer chain [8, 9, 12, 31]. Basically, for P3ATs emission spectra we may approximate the line shape considering quinone or oligomer structures (high energy) and pristine (low energy) structures. The main structures present in these polymers such as the quinone and pristine structures are shown in **Figure 3**. The result is the maximum shift or relative intensity change due to the interaction of electron-vibrational modes of quinone or pristine structures [8, 19] or different lengths of polymer chains [38].

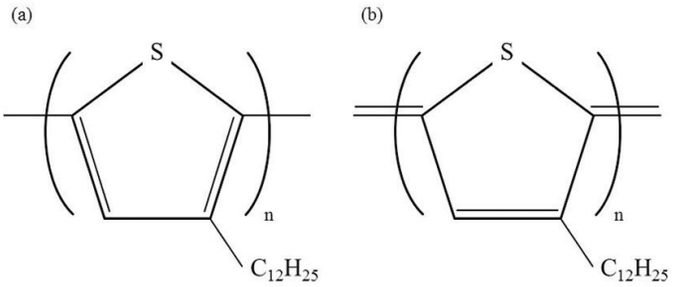

Figure 3. Scheme for P3DDT (a) pristine and (b) quinone structure.

Figure 4a and **b** shows the PL spectra of P3DDT film synthesized using both Et_4NBF_4 or $LiClO_4$ electrolytes, respectively. Note that the spectra are broad in the UV-Vis spectral range. **Figure 4a** shows normalized PL spectra for P3DDT films grown using the Et_4NBF_4 electrolyte, where the maximum of the emission redshift increased the number of cycles. This is due to the presence of oligomers with smaller conjugation lengths [38] and quinone chains [8, 19]. In addition for EtNBF01–EtNBF04 films, it is possible the occurrence of polymer chains with lower molecular weight and interface substrate/polymer, polymer/polymer and polymer/electrolyte effects [14, 22]. By increasing the film thickness (>4 cycles), PL spectra shifted to high wavelengths (*redshift*), it according the rise of in residence time in the electropolymerization process in the presence of higher conjugated polymer chains and pristine structures [8, 9, 12]. **Figure 4b** shows the PL spectra of P3DDT films synthesized with $LiClO_4$, presenting the similar line shape characteristics observed in **Figure 4(a)**. Film emission spectra utilizing that electrolyte also display different radiative processes. In this case, we consider two different configurations of P3DDT molecules, i.e., pristine or quinone structures [8, 9, 12]. The emission line shape is practically identical to LiClO01–LiClO08 films. However, the PL spectra for the thicker LiClO10 film is red shifted due to the new polymer structures created by the interaction ClO_4^- ion present in the solution [8, 12]. It is possible in the synthesis the presence of high

[2]PL measurements were obtained by exciting the samples with the 405 nm line of a diode laser at 4.0 mW (Laser LineiZi), vertically polarized in relation to the laboratory reference. The emission was detected and analyzed by a USB 2000 ocean optics spectrophotometer.

polymer conjugation length or pristine structures [8, 9, 12]. Results are coherent with recent observation of P3ATs when different electrolytes tend to influence the molecular polymer structure [7, 33].

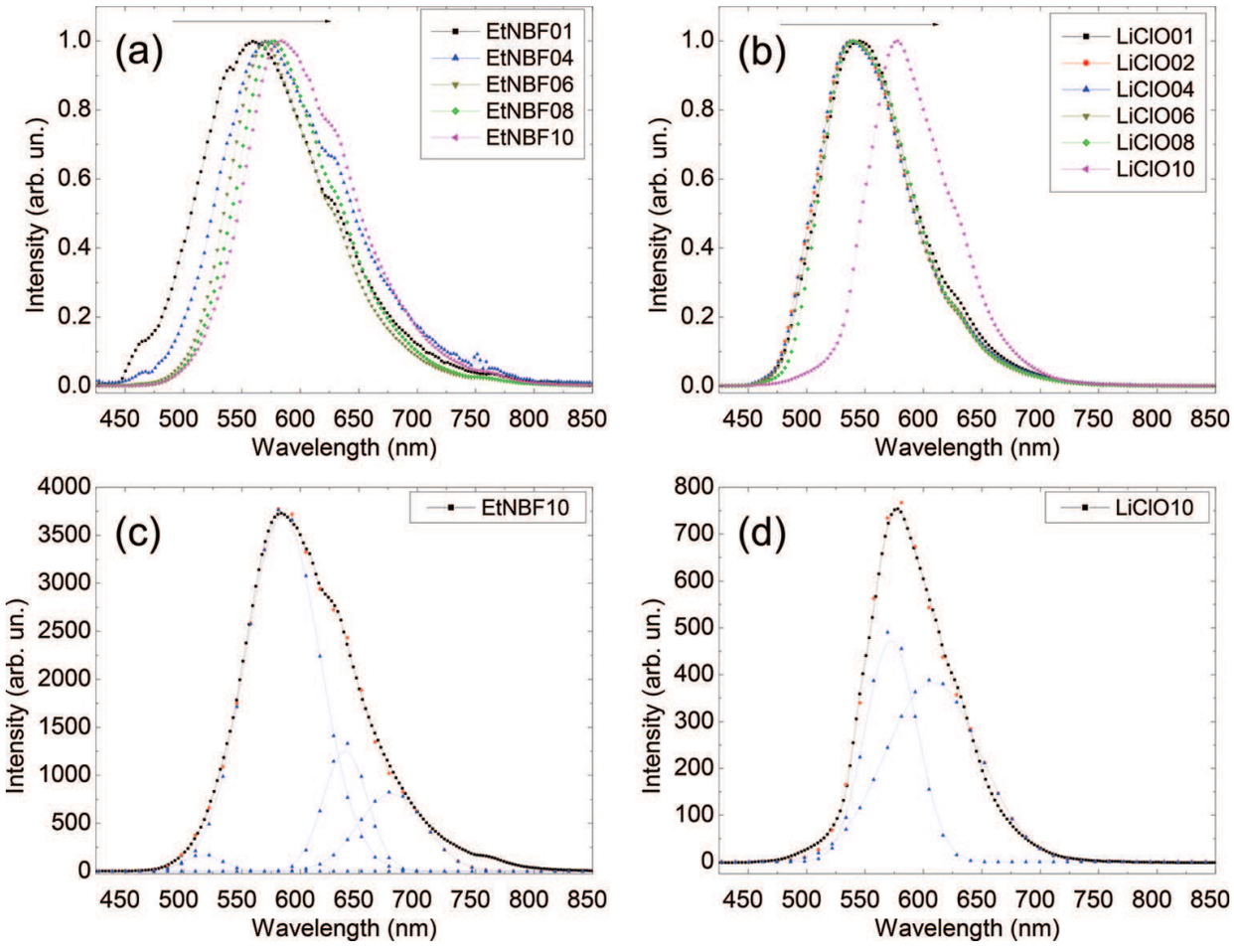

Figure 4. PL spectra for P3DDT films formed with electrolyte (a) Et4NBF4 and (b) LiClO4. PL simulation for (c) EtNBF10 and (d) LiClO10 films.

Figure 4(c) and **(d)** shows the spectra simulation for EtNBF10 and LiClO10 films, respectively, using the multi-Gaussian function, following the procedure utilized for P3AT polymers [8, 9, 12, 13]. First, we consider the polymer chains without the presence of dopants and without structural changes. Second, we introduce the contribution to the emission line shape of dopants and possible new structural changes (**Figure 3**) [8], as established by the P3AT family [35–37] in the energy range of polymeric chains or oligomers [38, 39]. Moreover, it was also added bands due to the interaction of the electron-vibrational modes. The typical optically active vibration mode is 1450 cm^{-1} for the C=C group [37]. In **Figure 4(c)**, the PL spectra centered at ~516 nm can be assigned to high conjugation polymer chains. The second band at ~584 nm is due to quinone structures, which is the result of interaction between the salt and the polymer chains. The band at ~638 nm is attributed to pristine without the salt-polymer interaction.

Finally, the last one at ~678 nm is normally reported as the vibrational replica [35–37]. We perform a similar procedure to simulate the spectra of P3DDT films processed with $LiClO_4$ and the results are presented in **Figure 4(d)**. Note in this case, the spectrum may be simulated with only Gaussians curves [8, 12]. The emission band at ~572 nm is assigned to the interaction between the electrolyte and the polymer chain forming mainly quinone structures and a band at ~610 nm is due to the pristine structure. That result is agreement with the reports on the P3ATs family [8, 9, 12, 19]. A similar simulation was performed for all samples analyzed and the results are shown in **Table 3**. And it observed that the films synthesized with Et_4NBF_4 have vibrational replicas at 680 nm. The presence of the bands assigned to the quinone and pristine structures is also evident for both electrolytes. As a result, it is possible to correlate the maximum emission spectral position to the amount of these structures in the polymeric film.

Table 2 shows that the P3DDT *band gap* should change, increasing the number of the deposition cycles. However, data in **Table 3** demonstrate that the emission of quinone or pristine chains does not change the spectral position, respectively, at 569 ± 7 and 631 ± 8 nm for films grown in Et_4NBF_4 and 538 ± 9 and 588 ± 7 nm for the films grown in $LiClO_4$. The redshift in the emission spectra is due to the emission bands of the pristine or quinone species. In addition, the present result shows how the use of electropolymerization is able to synthesize regular polymer chains, in which it is an important point when the reproducibility of polymeric layers is important, mainly to applied in an organic device area.

Films	1st oligomers band nm (eV)	2nd oligomers band nm (eV)	Quinone band nm (eV)	Pristine band nm (eV)	Vibrational replica nm (eV)
EtNBF01	465 (2.66)	520 (2.38)	568 (2.18)	630 (1.96)	684 (1.81)
EtNBF02	461 (2.68)	515 (2.40)	556 (2.22)	610 (2.03)	674 (1.83)
EtNBF04	–	500 (2.47)	569 (2.17)	638 (1.94)	691 (1.79)
EtNBF06	–	499 (2.48)	566 (2.19)	625 (1.98)	683 (1.81)
EtNBF08	–	512 (2.42)	575 (2.15)	632 (1.96)	675 (1.83)
EtNBF10	–	516 (2.40)	584 (2.12)	638 (1.94)	678 (1.82)
LiClO01	–	–	540 (2.29)	589 (2.10)	–
LiClO02	–	–	539 (2.30)	588 (2.10)	–
LiClO04	–	–	537 (2.30)	587 (2.11)	–
LiClO06	–	–	535 (2.31)	579 (2.14)	–
LiClO08	–	–	534 (2.32)	576 (2.15)	–
LiClO10	–	–	572 (2.16)	608 (2.03)	–

Table 3. Maximum of curves of the deconvolution in the PL spectra for EtNBFxx and LiClOxx films.

3.3. Emission ellipsometry (EE)[3]

Recently, we demonstrated the correlation between polarized emission light and P3DDT films grown using the electrochemical using emission ellipsometry technique [25, 26, 40]. Photoluminescence polarization reveal important properties of the material structure, e.g., anisotropy, which has immediate application in industry [41]. By using the ellipsometry technique, the polarization state of the emitted light can be determined by calculating the S_0, S_1, S_2 and S_3 Stokes parameters. S_0 is associated with the total light emitted amount, S_1 describes the linearly polarized amount of light in the vertical or horizontal direction, S_2 describes the linear polarization amount rotated by +45° or -45° and S_3 describes the circularly polarized light to the right or left. These parameters are obtained by adjusting the intensity I of the equation [25, 40]:

$$I(\theta) = \frac{1}{2}\left[A + B\,.\,\sin(2\theta) + C\,.\,\cos(4\theta) + D\,.\,\sin(4\theta)\right] \tag{2}$$

where I is the electric field intensity, θ is the angle between the axes of the quarter-wave plate and of the polarizer, $A = S_0 - \frac{S_1}{2}$, $B = S_3$, $C = -\frac{S_1}{2}$ and $D = -\frac{S_2}{2}$, where S_0, S_1, S_2 and S_3 are the Stokes parameters. In practice, the quarter-wave plate is rotated by discrete angles θ_j such that:

$$\begin{aligned} A &= \frac{2}{N}\sum_{n=1}^{N} I\left(n\,\theta_j\right) \\ B &= \frac{4}{N}\sum_{n=1}^{N} I\left(n\,\theta_j\right)\sin\left(2n\,\theta_j\right) \\ C &= \frac{4}{N}\sum_{n=1}^{N} I\left(n\,\theta_j\right)\cos\left(4n\,\theta_j\right) \\ D &= \frac{4}{N}\sum_{n=1}^{N} I\left(n\,\theta_j\right)\sin\left(4n\,\theta_j\right) \end{aligned} \tag{3}$$

where N is the number of steps of the quarter-wave plate. Eq. [2] can be solved considering the eight possible combinations of the harmonic functions (sine and cosine) and the total intensity (parameter S_0). In other words, the minimum number of points for solving Eq. (2) is $N = 9$ or $\Delta\theta = 40°$ and, from the experimental point of view, the symmetry $I(\theta) = I(\theta + 2\pi)$. The new method to solve Eq. (2) was introduced by Basílio [42]. Stokes parameters are associated with the degree of polarization (P) of the emitted light by [25, 40]:.

$$P = \frac{\left(S_1^2 + S_2^2 + S_3^2\right)^{\frac{1}{2}}}{S_0}. \tag{4}$$

Moreover, it is also possible to obtain the dissymmetry factor g the circularly polarized light emission degree and the anisotropy factor r, it is associated with molecular ordering of the

[3]The emission ellipsometry experiment was performed using the setup described by Alliprandini et al. [25–27]. The samples were excited by a laser in 405 nm, and the emitted light was collected by a set of lenses and directed through an achromatic quarter-wave-plate (Newport 10RP54-1), as a compensator and an achromatic polarizer (Newport 10LP-VIS-B). The emission was detected and analyzed by an USB 2000 Ocean Optics spectrophotometer. The experiment was performed by rotating the compensator in its own plane from 0 rad (0°) to ~6.28 rad (360°), with steps of ~0.17 rad (10°). All measurements were performed at room temperature (~20°C) and under 10-4 Torr vacuum.

http://dx.doi.org/10.5772/66921

polymer chains [22, 43]. These factors are obtained from the Stokes parameters in Eqs. (5) and (6). The use of the dissymmetry factor g equation is conditioned to the referential adopted: the vertical direction (y-axis) as a positive sign and the horizontal direction (x-axis) as a negative sign.

$$g = \pm 2\frac{S_3}{S_0} \tag{5}$$

$$r = \frac{-2\frac{S_1}{S_0}}{3+\frac{S_1}{S_0}} \tag{6}$$

3.3.1. Emission ellipsometry in P3DDT

The results presented in this section are dedicated to study the photophysical effects of P3AT films. In addition, it is possible to correlate the energy transfer mechanisms [44, 45] and polarization light states [22, 25–27]. Note that, in general, they are intrinsic characteristics semiconductor polymers. Stokes parameters are directly related to the light polarization states and, consequently, with factors related to orientation of the polymer chains in the films [25, 26], in which it provides information about the samples molecular ordering along the polymer films. In principle, the electrochemically synthesis by cyclic voltammetry does not show a molecular order [9].

Figure 5 shows the parameters S_1/S_0, S_2/S_0 and S_3/S_0 in the spectral range of P3DDT emission obtained from the EE data for EtNBF01 and EtNBF10 films. The Stokes parameter values are virtually null in **Figure 5a**. It indicates that the light emitted by EtNBF01 films has random polarizing directions, i.e., depolarized with high probability of energy transfer from the photoexcited carriers in all directions of the polymeric film plane. It is important to remember that the excitation polarization is linear in the vertical direction (laboratory referential) and only chronophers with transition dipole in the parallel direction are excited. However, for EtNBF10 film thickness, we observe, in **Figure 4b** significant variation for the S_1/S_0 and S_2/S_0 parameters. In principle, the films grown using electrochemical techniques have not molecular order [40], but they may have partially polarized emission when the excitation light is linearly polarized [9, 24, 40, 43]. Another important observation is that the inversion signal of the S_1/S_0 curve occurs simultaneously with the reversal of S_2/S_0 curve. This may be explained, according to Foster's energy transfer process mechanism [44] by the excitation low molecular weight chains or oligomers that have their transition electric dipole or part thereof aligned with the excitation source, energy absorbing (405 nm). Thus, part of the absorbed light is transferred via Förster processes to another polymer with larger conjugation length, pristine and quinone structures, in a random direction, depolarized and decreasing the values of the S_1/S_0 factor close to zero above 525 nm. However, some excited oligomers and low molecular weight chains may not energy transfer increasing the emission in the parallel direction of excitation polarized light [9, 26]. It is observed in the S_1/S_0 factor from 475 to 525 nm spectral range due to the effects of the substrate-polymer or polymer-polymer interface [14, 22]. Finally, the S_3/S_0 parameter indicates that the light emitted does not have significant right or left circular polarization.

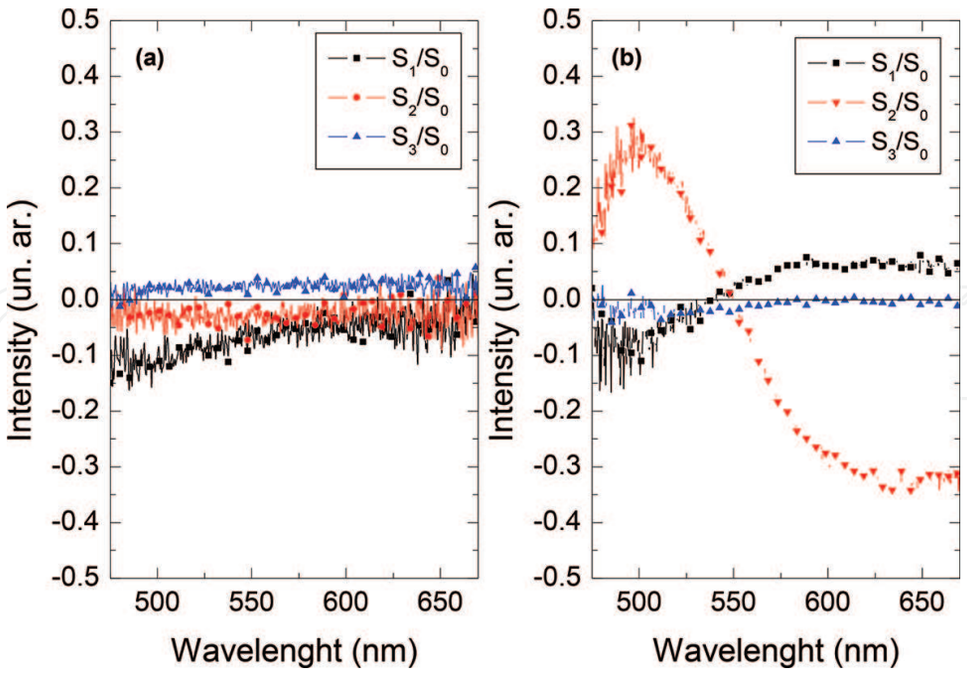

Figure 5. EE curves for films (a) EtNBF01 and (b) EtNBF10.

Förster energy transfer occurs when two conditions are met [44, 45]. First (i), the distance between the donor and the acceptor chromophores is up to ~ 10 nm, and (ii) second, parallelism condition, i. e, the electric dipole moment of the donor and the acceptor is parallel (aligned) or component of electric dipole moment of the acceptor is in the parallel direction of electric dipole moment of the donor [44]. Thus, when conjugated polymer segments absorb energy partially or totally is transferred to another, generally, higher conjugation polymer degree due to the electronic-vibrational relaxation mechanism. During the transfer process, the energy undergoes depolarization or rotational changes due to the misalignment of the dipoles in the same direction of the polymer main chains. As a result, when there is an emission in another part of the polymer or different polymer chains, a different polarization compared to the initial direction of the excitation polarization is obtained. Thus, the molecules, whose dipole or parts of its components are aligned with the excitation source, transfer energy to the polymers with greater conjugation lengths, causing an emission at lower energies. For the thick film in **Figure 5b**, the oligomers show great probability to transfer energy to other chains with greater conjugation lengths (quinone and pristine chains), parameter S_1/S_0 ~0, see spectral range assigned to oligomers between 475 and 525 nm. Similarly, **Figure 6** shows the EE curves for LiClO01 (**Figure 6a**) and LiClO10 (**Figure 6b**) films. Note that the emission of these films has horizontal and linear polarization, $S_1/S_0 > 0$ and polarization rotation to + 45° in relation to the polarization of the excitation light $S_2/S_0 < 0$. Circular polarization emission is not observed at S_3/S_0~0 to 500–675 nm. All samples processed using $LiClO_4$ have the same EE curves characteristics (**Figure 6**). An explanation for the absence of reverse bias directions and rotation observed for the films processed using the Et_4NBF_4 electrolyte is the preferential

http://dx.doi.org/10.5772/66921

formation of polymer chains with smaller conjugation lengths. It is compatible with the lower energy transfer at a higher spectral range <550 nm.

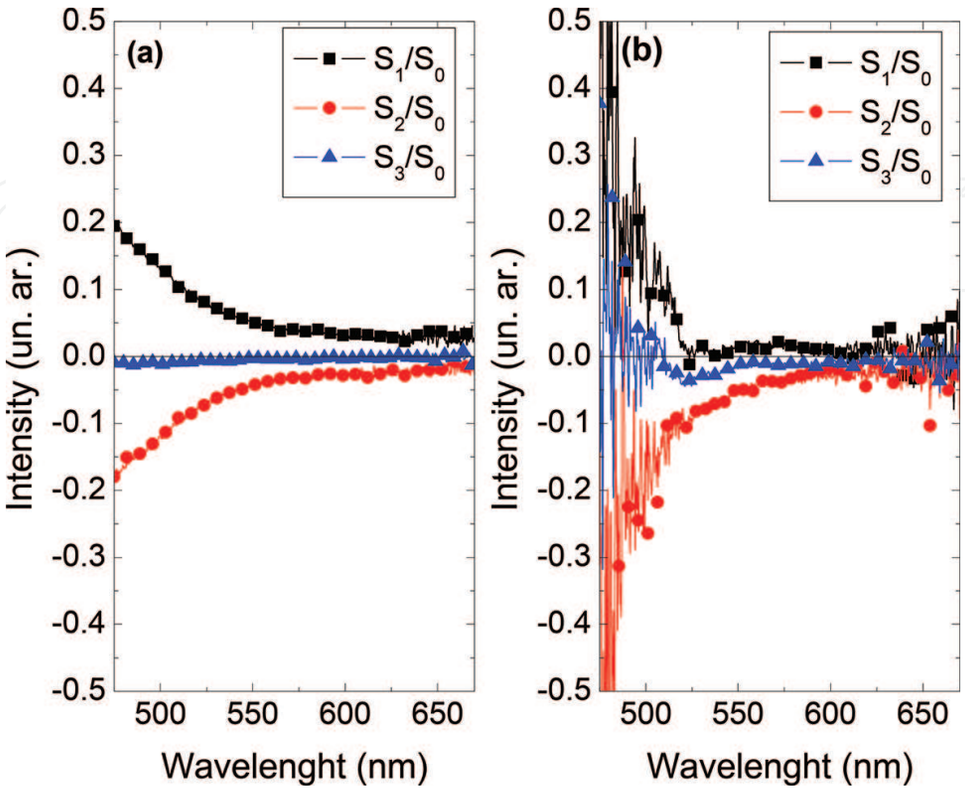

Figure 6. EE curves for films (a) LiClO01 and (b) LiClO10.

The polarization degree *P* (Eq. (4)) indicates the amount of light that is polarized, without differentiating between linearly or circularly polarized lights [25, 27, 40]. There are other two important parameter to quantify the polarization: the anisotropy factor *r* (Eq. (6)) that may be correlated with the direction of the polymer chains and the dissymmetry factor *g* (Eq. (5)) associated with the emission of the circularly polarized light [22, 40, 43]. The parameters *P*, *r* and *g* are obtained directly from Stokes parameter values [22, 43]. **Figures 5a** and **7a** show the polarization degree parameters for the EtNBF10 film in the function of the emission wavelength, presenting maximum at 495 and 630 nm. At 495 nm, we observe the signal inversion of S_2/S_0 coinciding with the minimal value for S_1/S_0 curves. The dissymmetry factor *g* in the emission spectral region is around ~5% or below, indicating that there is no emission of circularly polarized light [44]. **Figure 5b** shows the polarization degree *P*, anisotropy factors *r* and dissymmetry factor *g* for the LiClO10 film. We can observe that the polarization of the emitted light is high (~28%) at a low wavelength region (<550 nm) addressed with oligomers decreasing monotonic above 550 nm. The parameters *r* and *g* followed the spectral dependence of *p*. However, the parameter *g* does not display significant values. On the other hand, *r* values in the spectral range of oligomers emission are related to the decrease of energy transfer between adjacent polymer chain, according to reference [26]. The dissymmetry factor *g* has no significant intensity.

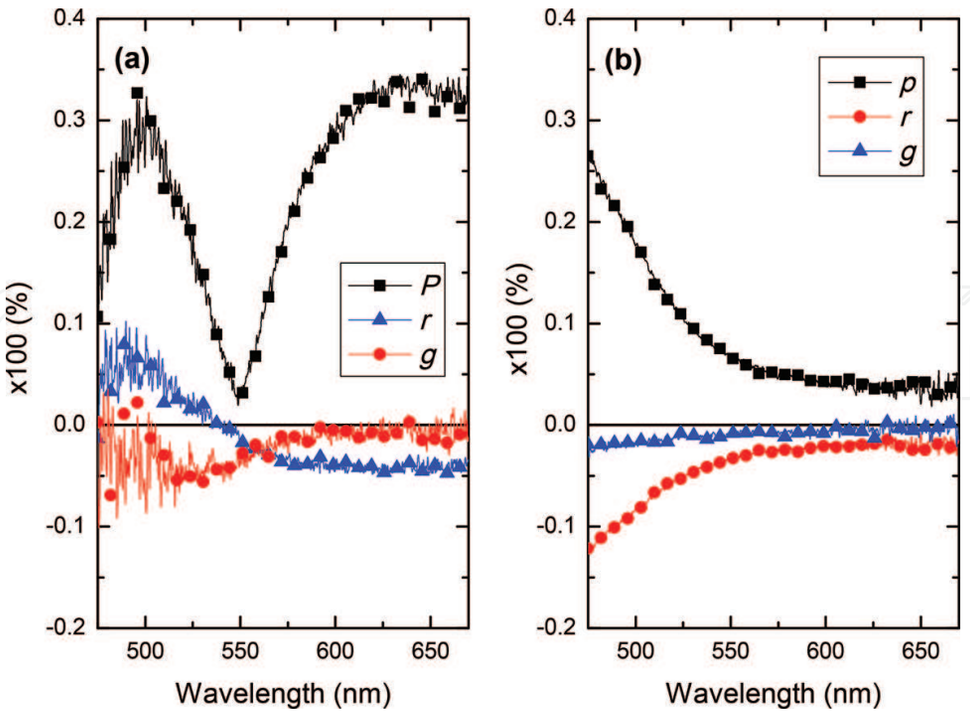

Figure 7. Polarization degree *P*, anisotropy factor *r* and dissymmetry factor *g* obtained from the Stokes parameters for the (a) EtNBF10 film and (b) LiClO10 film.

4. Conclusions

We showed the strong correlation between the optical properties of a P3AT polymer and the conditions of the polymer electrochemical growth, demonstrating that it is possible to control the optical properties of polymeric films by controlling the growth conditions. For this, we use different electrolytes during the synthesis of polymeric films, which were linked to the number of growing cycles, according to the cyclic voltammetry electrochemical technique. Electrochemical synthesis is shown in efficient growth polymeric films when the concentrations of the reagents are equilibrated, e.g., the concentration for electropolymerization of the P3DDT occurs homogeneously with 0.050 mol L^{-1} monomer and 0.100 mol L^{-1} of $LiClO_4$. Furthermore, it is possible to measure the energy gap E_g for organic semiconductor directly from the cyclic voltammogram.

Through the UV-Vis results, it is possible to conclude that the electrolytes reacted differently in this material, shifting the spectrum to other regions of absorption as occurs to electrolyte change. PL results showed the existence of several contributions in each spectrum, in which the highest intensity contributions, quinone and pristine are the result of two structures that the polymer chains can take through the interactions between each electrolyte/polymer. These contributions are able to shift the maximum emission in each spectrum when the film thickness increases, and more effectively for the films containing Et_4NBF_4. There are also contributions resulting from the oligomers emission and the electron-phonon interactions. The EE demonstrated energy transfer processes by the Förster mechanism, where the emission polarization is observed and this has gradually changed with increasing emission wavelength. However, it is an isotropic material when obtained for CV, shown by the anisotropy factor, *r*. These

analyses show that the Förster *energy transfer process* occurs in this material and is responsible for the emission throughout the spectral window. Furthermore, more accentuated emissions polarization can be related to the oligomer emission.

Results show that the P3ATs deposited electrochemically has great potential for application in optoelectronic organic devices since P3ATs optical properties can be easily adjusted by controlling the deposition. In addition, results also showed the great light absorption capacity and a broad spectral window for the P3DDT emission. Moreover, it is also observed the presence of electron-phonon combination, which can contribute to the occurrence of energy transfer or charge transfer significantly, enhancing the use of P3DDT in optoelectronic devices, which makes this promising material to form the active layer of multiple devices, such as organic light emitting diodes (OLEDs), photovoltaics, photodetectors and mobile devices screens (displays), among others.

Acknowledgements

The authors are grateful to the following Brazilian Agencies: FAPEMIG, CAPES, CNPQ and FUFMT.

Author details

Sankler Soares de Sá[1], Fernando Costa Basílio[2], Henrique de Santana[3], Alexandre Marletta[2] and Eralci Moreira Therézio[4]*

*Address all correspondence to: therezio@ufmt.br

1 Institute of Agricultural and Technology Science, Federal University of Mato Grosso, Rondonópolis, Brazil

2 Physics Institute, Federal University of Uberlândia, Uberlândia, Brazil

3 Chemistry Department, State University of Londrina, Londrina, Brazil

4 Institute of Exact and Natural Sciences, Federal University of Mato Grosso, Rondonópolis, Brazil

References

[1] Bundgaard E, Krebs FC. Low band gap polymers for organic photovoltaics. Solar Energy Materials and Solar Cells. 2007;**91**(11):954–985. DOI: 10.1016/j.solmat.2007.01.015

[2] Fujii A, Kawahara H, Yoshida M, Ohmori Y, Yoshino K. Emission enhancement in electroluminescent diode utilizing poly(3-alkylthiophene) doped with oxadiazole derivative. Journal of Physics D: Applied Physics. 1995;**28**(10):2135.

[3] Valaski R, Moreira LM, Micaroni L, Hümmelgen IA. The electronic behavior of poly(3-octylthiophene) electrochemically synthesized onto Au substrate. Brazilian Journal of Physics. 2003;**33**:392–397. DOI: 10.1590/S0103-97332003000200043

[4] Wang G, Yuan C, Lu Z, Wei Y. Enhancement of organic electroluminescent intensity by charge transfer from guest to host. Journal of Luminescence. 1996;**68**(1):49–54. DOI: 10.1016/0022-2313(95)00092-5

[5] Yoshino K, Manda Y, Sawada K, Onoda M, Sugimoto Ri. Anomalous dependences of luminescence of poly(3-alkylthiophene) on temperature and alkyl chain length. Solid State Communications. 1989;**69**(2):143–146. DOI: 10.1016/0038-1098(89)90379-7

[6] Ohmori Y, Uchida M, Muro K, Yoshino K. Visible-light electroluminescent diodes utilizing poly(3-alkylthiophene). Japanese Journal of Applied Physics. 1991;**30**(11B):L1938. DOI: 10.1143/JJAP.30.L1938

[7] Roncali J. Conjugated poly(thiophenes): synthesis, functionalization and applications. Chemical Reviews. 1992;**92**(4):711–738. DOI: 10.1021/cr00012a009

[8] Therézio EM, Duarte JL, Laureto E, Di Mauro E, Dias IL, Marletta A, et al. Analysis of the optical properties of poly(3-octylthiophene) partially dedoped. Journal of Physical Organic Chemistry. 2011;**24**(8):640–645. DOI: 10.1002/poc.1802

[9] Therézio EM, Franchello F, Dias IFL, Laureto E, Foschini M, Bottecchia OL, et al. Emission ellipsometry as a tool for optimizing the electrosynthesis of conjugated polymers thin films. Thin Solid Films. 2013;**527**:255–260. DOI:10.1016/j.tsf.2012.11.093

[10] Cervantes TNM, Bento DC, Maia ECR, Fernandes RV, Laureto E, Moore GJ, et al. The influence of different electrolytes on the electrical and optical properties of polymer films electrochemically synthesized from 3-alkylthiophenes. Journal of Materials Science: Materials in Electronics. 2014;**25**(4):1703–1715. DOI: 10.1007/s10854-014-1787-4

[11] Cervantes TNM, Bento DC, Maia ECR, Zaia DAM, Laureto E, da Silva MAT, et al. In situ and ex situ spectroscopic study of poly(3-hexylthiophene) electrochemically synthesized. Journal of Materials Science: Materials in Electronics. 2012;**23**(10):1916–1921. DOI: 10.1007/s10854-012-0880-9

[12] Maia ECR, Bento DC, Laureto E, Zaia DAM, Therézio EM, Moore JG, et al. Spectroscopic analysis of the structure and stability of two electrochemically synthesized poly(3-alkylthiophene)s. Journal of the Serbian Chemical Society. 2013;**78**(4):507–521. DOI: 10.2298/JSC120327111R

[13] Yoshino K, Hayashi S, Sugimoto R. Preparation and properties of conducting heterocyclic polymer films by chemical method. Japanese Journal of Applied Physics. 1984;**23**(12A):L899. DOI: 10.1143/JJAP.23.L899

[14] Therézio EM, Piovesan E, Anni M, Silva RA, Oliveira ON, Marletta A. Substrate/semiconductor interface effects on the emission efficiency of luminescent polymers. Journal of Applied Physics. 2011;**110**(4):044504. DOI: 10.1063/1.3622143

[15] Marletta A. Optical properties of organic semiconductors based on Light Emitting Polymers [thesis]. São Carlos: Universidade de São Paulo; 2001. DOI:10.11606/T.76.2001.tde-10022002-091803

[16] Therézio EM, Rodrigues PC, Tozoni JR, Marletta A, Akcelrud L. Energy-transfer processes in donor–acceptor poly(fluorenevinylene-alt-4,7-dithienyl-2,1,3-benzothiadiazole. Journal of Physical Chemistry C.2013;**117(**25):13173–13180. DOI: 10.1021/jp400823d

[17] Beaujuge PM, Amb CM, Reynolds JR. Spectral engineering in π-conjugated polymers with intramolecular donor-acceptor interactions. Accounts of Chemical Research. 2010; **43**(11):1396–1407. DOI: 10.1021/ar100043u

[18] van Mullekom HAM, Vekemans JAJM, Havinga EE, Meijer EW. Developments in the chemistry and band gap engineering of donor–acceptor substituted conjugated polymers. Materials Science and Engineering: R: Reports. 2001;**32**(1):1-40. DOI: 10.1016/S0927-796X(00)00029-2

[19] Therézio EM. Electrochemical synthesis, characterization and optical properties analysis of the poly (3-octylthiophene) (P3OT) [dissertation]. Londrina: Universidade Estadual de Londrina; 2009.

[20] Bento DC, Maia ECR, Cervantes TNM, Fernandes RV, Di Mauro E, Laureto E, et al. Optical and electrical characteristics of poly(3-alkylthiophene) and polydiphenylamine copolymers: applications in light-emitting devices. Synthetic Metals. 2012;**162**(24):2433–2442. DOI: 10.1016/j.synthmet.2012.12.006

[21] Kaur M, Gopal A, Davis RM, Heflin JR. Concentration gradient P3OT/PCBM photovoltaic devices fabricated by thermal interdiffusion of separately spin-cast organic layers. Solar Energy Materials and Solar Cells. 2009;**93**(10): 1779–1784. DOI: 10.1016/j.solmat.2009.06.009

[22] Therézio EM, Piovesan E, Vega ML, Silva RA, Oliveira ON, Marletta A. Thickness and annealing temperature effects on the optical properties and surface morphology of layer-by-layer poly(p-phenyline vinylene)+dodecylbenzenesulfonate films. Journal of Polymer Science Part B: Polymer Physics. 2011;**49**(3):206–213. DOI: 10.1002/polb.22180

[23] Therézio EM, Vega ML, Faria RM, Marletta A. Statistical Analysis in Homopolymeric Surfaces. In: Dr. Vijay Nalladega, editor. Scanning Probe Microscopy-Physical Property Characterization at Nanoscale. Rijeka: InTech; 2012. pp. 59–80. DOI: 10.5772/36461

[24] Marletta A, Vega ML, Rodrigues CA, Gobato YG, Costa LF, Faria RM. Photo-irradiation effects on the surface morphology of poly(p-phenylene vinylene) films. Applied Surface Science. 2010;**256**(10):3018-3023. DOI: 10.1016/j.apsusc.2009.11.066

[25] Alliprandini-Filho P, da Silva GB, Barbosa Neto NM, Silva RA, Marletta A. Induced secondary structure in nanostructured films of poly(p-phenylene vinylene). Journal of Nanoscience and Nanotechnology. 2009;**9**(10):5981–5989. DOI: 10.1166/jnn.2009.1293

[26] Alliprandini-Filho P, da Silva RA, Barbosa Neto NM, Marletta A. Partially polarized fluorescence emitted by MEHPPV in solution. Chemical Physics Letters. 2009;**469** (1–3):94–98. DOI: 10.1016/j.cplett.2008.12.057

[27] Alliprandini-Filho P, Silva RA, Silva GB, Barbosa Neto NM, Cury LA, Moreira RL, et al. Measurement of the emitted light polarization state in oriented and non-oriented PPV films. Macromolecular Symposia. 2006;**245–246**(1):406–409. DOI: 10.1002/masy.200651357

[28] Bento DC, Louarn G, de Santana H. Structural stability and improved properties of poly(3-alkylthiophenes) synthesized in an acid medium. Journal of Materials Science: Materials in Electronics. 2016;**27**(5):5371–5382. DOI: 10.1007/s10854-016-4437-1

[29] de Santana H, Maia ECR, Bento DC, Cervantes TNM, Moore GJ. Spectroscopic study of poly(3-alkylthiophenes) electrochemically synthesized in different conditions. Journal of Materials Science: Materials in Electronics. 2013;**24**(9):3352–3358. DOI: 10.1007/s10854-013-1254-7

[30] Silva TH, Barreira SVP, Moura C, Silva F. Electrochemical characterization of a self-assembled polyelectrolyte film. Portugaliae Electrochimica Acta. 2003;**21**(3):281–292.

[31] Bento DC, Maia ECR, Cervantes TNM, Olivati CA, Louarn G, de Santana H. C. Complementary study on the electrical and structural properties of poly(3-alkylthiophene) and its copolymers synthesized on ITO by electrochemical impedance and Raman spectroscopy. Journal of Materials Science: Materials in Electronics. 2015;**26**(1):149–161. DOI: 10.1007/s10854-014-2377-1

[32] Skompska M, Szkurłat A. The influence of the structural defects and microscopic aggregation of poly(3-alkylthiophenes) on electrochemical and optical properties of the polymer films: discussion of an origin of redox peaks in the cyclic voltammograms. Electrochimica Acta. 2001;**46**(26–27):4007–4015. DOI: 10.1016/S0013-4686(01)00710-1

[33] Obaid AY, El-Mossalamy EH, Al-Thabaiti SA, El-Hallag IS, Hermas AA, Asiri AM. Electrodeposition and characterization of polyaniline on stainless steel surface via cyclic, convolutive voltammetry and SEM in aqueous acidic solutions. International Journal of Electrochemical Science. 2014;**9**(2):1003–1015.

[34] Eckhardt H, Shacklette LW, Jen KY, Elsenbaumer RL. The electronic and electrochemical properties of poly(phenylene vinylenes) and poly(thienylene vinylenes): an experimental and theoretical study. The Journal of Chemical Physics. 1989;**91**(2):1303–1315. DOI: 10.1063/1.457153

[35] Österbacka R, An CP, Jiang XM, Vardeny ZV. Two-dimensional electronic excitations in self-assembled conjugated polymer nanocrystals. Science. 2000;**287**(5454):839. DOI: 10.1126/science.287.5454.839

[36] Kobayashi T, Hamazaki J-i, Kunugita H, Ema K, Endo T, Rikukawa M, et al. Coexistence of photoluminescence from two intrachain states in polythiophene films. Physical Review B. 2003;**67**(20):205214. DOI: 10.1103/PhysRevB.67.205214

[37] Kanemoto K, Sudo T, Akai I, Hashimoto H, Karasawa T, Aso Y, et al. Intrachain photoluminescence properties of conjugated polymers as revealed by long oligothiophenes and polythiophenes diluted in an inactive solid matrix. Physical Review B. 2006;**73**(23):235203. DOI: 10.1103/PhysRevB.73.235203

[38] Alves MRA, Calado HDR, Matencio T, Donnici CL. Thiophene-based oligomers and polymers: syntheses and applications. Química Nova. 2010;**33**(10):2165–2175. DOI: 10.1590/S0100-40422010001000029

[39] Chan HSO, Ng SC. Synthesis characterization and applications of thiophene-based functional polymers. Progress in Polymer Science. 1998;**23**(7):1167–1231. DOI: 10.1016/S0079-6700(97)00032-4

[40] Collet E. Polarized Light: Fundamentals and Applications. New York: Marcel Dekker; 1993. 581 p.

[41] Cimrová V, Remmers M, Neher D, Wegner G. Polarized light emission from LEDs prepared by the Langmuir-Blodgett technique. Advanced Materials. 1996;**8**(2):146–149. DOI: 10.1002/adma.19960080209

[42] Basílio FC. Implementation of the New Technique Raman Spectroscopy by Elipsometry no Chiral Molecules Study [dissertation]. Uberlândia: Universidade Federal de Uberlândia; 2014.

[43] Therézio EM, da Silva SFC, Dalkiranis GG, Alliprandini Filho P, Santos GC, Ely F, et al. Light polarization states of a cholesteric liquid crystal probed with optical ellipsometry. Optical Materials. 2015;**48**:7–11. DOI: 10.1016/j.optmat.2015.07.010

[44] Förster T. Intermolecular energy migration and fluorescence. Annalen der Physik. 1948;**437**(1–2):55–75.

[45] Dexter DL. Cooperative optical absorption in solids. Physical Review. 1962;**126**(6):1962–7.

IntechOpen